



European Union's Seventh Framework Programme
Grant Agreement №: 603521

Project Acronym: **PREFACE**

Project full title: **Enhancing prediction of tropical Atlantic climate and its impacts**

Instrument: Collaborative Project

Theme: ENV.2013.6.1-1 – *Climate-related ocean processes and combined impacts of multiple stressors on the marine environment*

Start date of project: 1 November 2013

Duration: 48 Months

Deliverable Reference Number and Title:

D 9.2

"Mechanisms for long-term TAV"

Lead work package¹ for this deliverable: WP9

Lead contractor¹ for this deliverable: CERFACS

Due date of deliverable: 31/10/2015

Actual submission date:

Project co-funded by the European Commission within the Seven Framework Programme (2007-2013)		
Dissemination Level		
PU	Public	PU
PP	Restricted to other programme participants (including the Commission Services)	
RE	Restricted to a group specified by the Consortium (including the Commission Services)	

¹ Name of beneficiary (=institute/organisation/university)

CO	Confidential, only for members of the Consortium (including the Commission Services)	
-----------	--	--

Contribution to project objectives – with this deliverable, the project has contributed to the achievement of the following objectives (see Annex I / DOW, Section B1.1.):

N. ^o	Objective	Yes	No
1	Reduce uncertainties in our knowledge of the functioning of Tropical Atlantic (TA) climate, particularly climate-related ocean processes (including stratification) and dynamics, coupled ocean, atmosphere, and land interactions; and internal and externally forced climate variability.	X	
2	Better understand the impact of model systematic error and its reduction on seasonal-to-decadal climate predictions and on climate change projections.		X
3	Improve the simulation and prediction TA climate on seasonal and longer time scales, and contribute to better quantification of climate change impacts in the region.		X
4	Improve understanding of the cumulative effects of the multiple stressors of climate variability, greenhouse-gas induced climate change (including warming and deoxygenation), and fisheries on marine ecosystems, functional diversity, and ecosystem services (e.g., fisheries) in the TA.	X	
5	Assess the socio-economic vulnerabilities and evaluate the resilience of the welfare of West African fishing communities to climate-driven ecosystem shifts and global markets.		X

Authors of this deliverable:

E. Sanchez-Gomez¹ and E. Mohino²

¹ CERFACS, Toulouse, France

² UCM, Madrid, Spain

List of beneficiaries

No	Name	Short Name
1	UNIVERSITETET I BERGEN	UiB
3	CENTRE EUROPEEN DE RECHERCHE ET DE FORMATION AVANCEE EN CALCUL SCIENTIFIQUE	CERFAC S
15	FUNDACIO INSTITUT CATALA DE CIENCIES DEL CLIMA	IC3

16	UNIVERSIDAD COMPLUTENSE DE MADRID	UCM
27	UNIVERSITY OF NIGERIA	UNN

Deviation from planned efforts for this deliverable:

(PLEASE ONLY COMMENT IF THERE WERE DEVIATIONS FROM THE ORIGINAL PLAN² IN PERSON-MONTHS PER BENEFICIARY¹ AND/OR WORK PACKAGE OR OTHER RESOURCE USE FOR ACHIEVEMENT OF THIS DELIVERABLE)

There has been a minor deviation from the original plan for beneficiary UNN (27). Research in the framework of task 9.2 suggested the existence of decadal variability in the Atlantic cold tongue, which had not been explicitly addressed in the DOW. UNN (27) in collaboration with UiB (1) looked further into this key issue. UNN devoted approximately 12 PMs, which were transferred from WP8. This was possible because UCM took the lead on D8.1.

Report on the deliverable:

(SHORT DESCRIPTION OF WORK PERFORMED; MAIN RESULTS ACHIEVED; CONTRIBUTION TO WP OBJECTIVES and TASKS)

Contribution to WP objectives and tasks:

The main goal of WP9 is to improve our understanding of Tropical Atlantic variability and its impacts through the analysis of observational data and climate model simulations.

D9.2 contributes to the second specific objective of WP9:

- To understand the long-term variations in the Tropical Atlantic addressing the relative roles of external forcings and internal variability, and task 9.2 (understanding of long-term variability in the Tropical Atlantic).

Introduction:

Decadal to multi-decadal variations in the Tropical Atlantic (TA) are caused by low-frequency internal processes and changes in external influences. These external influences can be natural in origin, such as volcanic activity and variations in solar output, or caused by human activity, such as greenhouse gas emissions (GHGs), human-sourced aerosols and land use change. Delineating the relative role of anthropogenic forcing, natural forcing, and long-term internal variability in the climate evolution during the last past 50 years presents a significant scientific challenge.

PREFACE (D9.2) has undertaken a number of works aimed at: 1) characterising the observed variability in the TA by working on the past-Atlantic low-frequency variations by

² See [List of person-months, nature and dissemination level of deliverable](#)

using marine proxies; 2) understanding the role of the different factors (internal, external) affecting the low-frequency variability in the TA; and 3) investigating physical processes governing the internal variability.

1. Characterisation of observed long-term climate variability

N. Keenlyside¹, L. Svendsen²

¹ *UiB, Bergen, Norway*

² *NERSC, Bergen, Norway*

(Svendsen et al. 2014)

Studies suggest that the Atlantic Multi-decadal Variability (AMV) is important for climate variability globally and has been connected to several regional climate signals. The AMV and the TA variability are related: In the TA the AMV can, for instance, affect the frequency of Atlantic hurricanes (Goldenberg et al., 2001) and the rainfall in the African Sahel (Zhang and Delworth, 2006; Wang et al., 2012). Recently, it is has been shown that the AMV can modulate the teleconnections between the Atlantic-Pacific Niños (Martin-Rey et al. 2014).

The problem is that ocean temperature data are limited to the last 140 years by instrumental records, hence the relatively short instrumental sea surface temperature (SSTs) record can therefore only capture 1–2 cycles of AMV, and is too short to confidently study natural low-frequency variability. Previous reconstructions of the AMV have mainly used land-based proxies, such as tree rings (Gray et al. 2004; Mann et al., 2009). The problem here is that the relationship between SST and land-based proxies seems strong for the instrumental era, but this relationship may not be stable. Therefore, we investigate low-frequency variability of North Atlantic SST using marine-based proxies, as these are a more direct measure of SST compared to land-based proxies. Here we propose a different method for reconstructing low-frequency variability in North Atlantic SST based on records from long-lived marine biota. We combine several annual resolution marine-based proxy records, extending 90 years further back in time than the instrumental record, with Principal Component Analysis (PCA) to extract the low-frequency variability and limit micro-environmental effects and sampling errors.

Figure 1 shows the PC1 of our reconstruction, together with the AMV-index from HadISST observations (Rayner et al. 2003). We also compare our results with two other AMV reconstructions (Gray et al., 2004; Mann et al., 2009), what are land-based multi-proxy reconstructions.

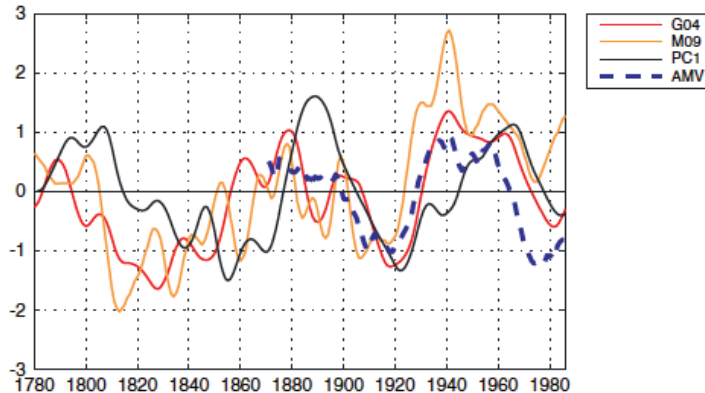


Figure 1. Normalized decadally filtered PC1 (solid black line), AMV reconstructions from Gray et al. [2004] (G04, red line) and Mann et al. [2009] (M09, orange line), and the AMV-index from HadISST data (dashed blue line). From Svendsen et al. 2013.

From figure 1 we find that PC1 is consistent with the observed AMV, and that the AMV persists throughout the record. This suggests that our method is able to capture the Atlantic low-frequency variability, and we conclude that this method is adequate for reconstructing SST on multidecadal timescales. There is a discrepancy in the timing of the variability between our marine-based reconstruction and other land-based multi-proxy AMV reconstructions, with the land-based AMV reconstructions leading the marine-based reconstruction by 11–12 years, indicating that we have to be careful about using proxies for reconstructing multidecadal SST variability in the Atlantic. From figure 1 it is clear that AMV oscillates on a 70-80 year timescale prior to the instrumental period (1870 to present). Thus, while external forcing of anthropogenic origin may have contributed to AMV during the historical period, it is not essential to generating it.

To conclude, we created the first marine-based proxy reconstruction of AMV. The index extended back to 1781 and revealed another 70-80 year cycle (Svendsen et al. 2014). Previous proxies have either been land based or derived from single records. Our reconstructions can also be used to investigate the persistence of observed AMV teleconnections in the TA. This record is freely available for use.

2. Role of internal variability versus external forcings:

F. Doblas-Reyes¹, N. Keenlyside², L. Svendsen³, L. Terray⁴, D Volpi¹

¹ IC3, Barcelona, Spain

² UiB, Bergen, Norway

³ NERSC, Bergen, Norway

⁴ CERFACS, Toulouse, France

Distinguishing between external (generally anthropogenic) and internal influences on time scales less than 50 years and spatial scales smaller than continental remains an

outstanding issue (IPCC 2007, 2013). The main objective of our work is to assess the role of internal variability versus the response to external forcings in long-term trends of SST, air temperature and precipitation in the tropical Atlantic and adjacent continents. Furthermore, we want to address whether the AMV, closely connected to TA decadal variability, can impact other regions outside the Atlantic, and if this relation is affected by external forcings. On this purpose, we have dealt with three different complementary approaches: a) in the first approach we use a huge ensemble of simulations (30 members) performed with the same climate model to separate the signal (external forcing) and the internal variability (residual variability) for explaining the trends in air temperature and precipitation in the TA; b) the second approach is based on the analysis of the decadal hindcasts from the CMIP5 (Coupled Model Intercomparison Project Phase 5, Taylor et al. 2012) multi-model ensemble; and in the third approach (c), we assess the role of the AMV in the early 20th Century warming and the relationship between the AMV and the Indian Summer Monsoon (IMS) from observations and CMIP5 models and transient simulations with the NorESM model.

a) The study of the respective roles of the internal versus the forced (external) variability in climate trends is usually carried out using data sets coming from CMIP5 models. This can be arguable, since most CMIP5 models contain too few realizations to adequately estimate the forced response on local/regional scales (Deser et al., 2012). Note that while it is common practice to average single runs from multiple models to obtain a robust estimate of anthropogenic climate change (e.g., the “multi-model mean”; IPCC, 2013), this approach does not allow the forced and unforced components of the response to be isolated in any given model.

Here instead we use a new 30-member initial-condition ensemble (CESM-LE) conducted with the National Center for Atmospheric Research (NCAR) Community Earth System Model version 1 (CESM1; Kay et al., 2014) covering the period 1920-2100 to the understanding of observed climate trends, with a particular focus on surface air temperature (SAT) and precipitation (PR) over the Tropical Atlantic during the past 63 years. Configured at a spatial resolution of 1° latitude/longitude (approximately 85 km at 40°N), this ensemble provides a perfect framework for the interpretation of nature’s one realization: specifically, the relative importance of internal variability and external radiative forcing at local/regional scales. As we have a 30-member ensemble, the ensemble mean provides a straightforward and good estimate of the forced response. Removing the forced response to individual members then leads to estimation of internal variability in each of the thirty members.

We are focusing here on the 1950-2012 period where previous studies have found a significant weakening trend of the equatorial Atlantic cold tongue (Tokinaga and Xie 2011). These authors find that «sea surface temperature has increased across the basin, with a local enhancement over the eastern equatorial Atlantic. This warming pattern of the sea surface is most pronounced during boreal summer, reducing the annual cycle through a positive ocean-atmosphere feedback». Enhanced atmospheric convection in the equatorial eastern Atlantic region and related weakened trade winds deepen the thermocline in the east, and reinforce the sea surface warming pattern. This study focused mostly on observations and

could not achieve a rigorous separation between the forced response and internal variability.

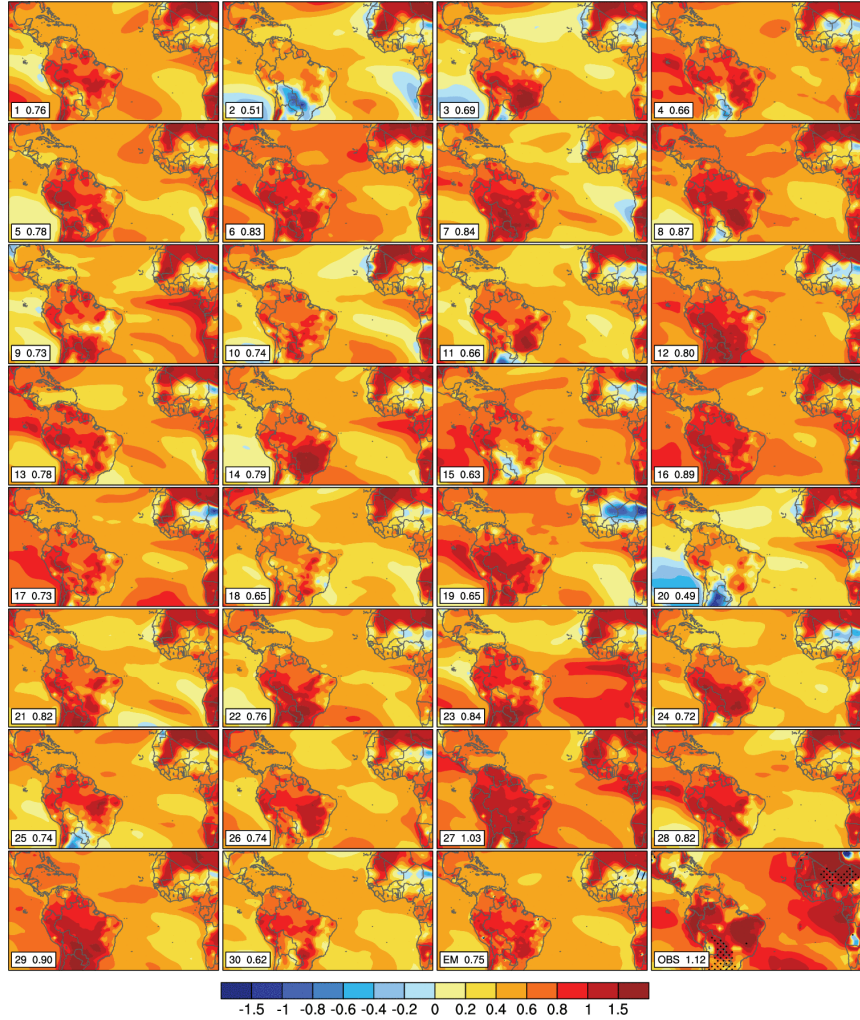


Figure 2. Summer surface air temperature trends (1950-2012; $^{\circ}\text{C } 63\text{yr}^{-1}$) for each of the CESM1 members (labelled 1-30), the CESM-LE ensemble mean (labelled EM) and the observations (here GISSTEMP, labelled OBS). The hatching in the EM panel denotes regions where less than 75% of the members agree on the sign of the trend. The stippling in the OBS panel shows regions where the amplitude of the EM trend is less than 1.5 standard deviation of the intra-ensemble trends. The numbers in each panel show the mean land warming of the region seen in the maps.

Figure 2 shows the 30 1950-2012 summer surface air temperature trends of the CESM-LE as well as the ensemble mean (the forced response) and the observations (GISSTEMP dataset). Note that the 30 trends differ only because of unpredictable internal variability due to the chaotic nature of climate at multi-decadal time scales. From figure 2 one can readily see that the evolution can be very different just due to internal variability. For example, members 9, 14 and 23 all exhibit an increased warming in the equatorial eastern Atlantic like the observations. They contrast with members 2, 7 and 19 that exhibit a

weak warming there and even a cooling in the southeast Atlantic. However, the forced response also shows a small increase of the warming in the eastern Atlantic compared to an almost uniform pattern elsewhere. The amplitude of the forced response is much smaller than the observed one (and the spatial pattern is quite different) suggesting that internal variability does have an important influence on the observed multi-decadal trends. This is also true for the other seasons (not shown).

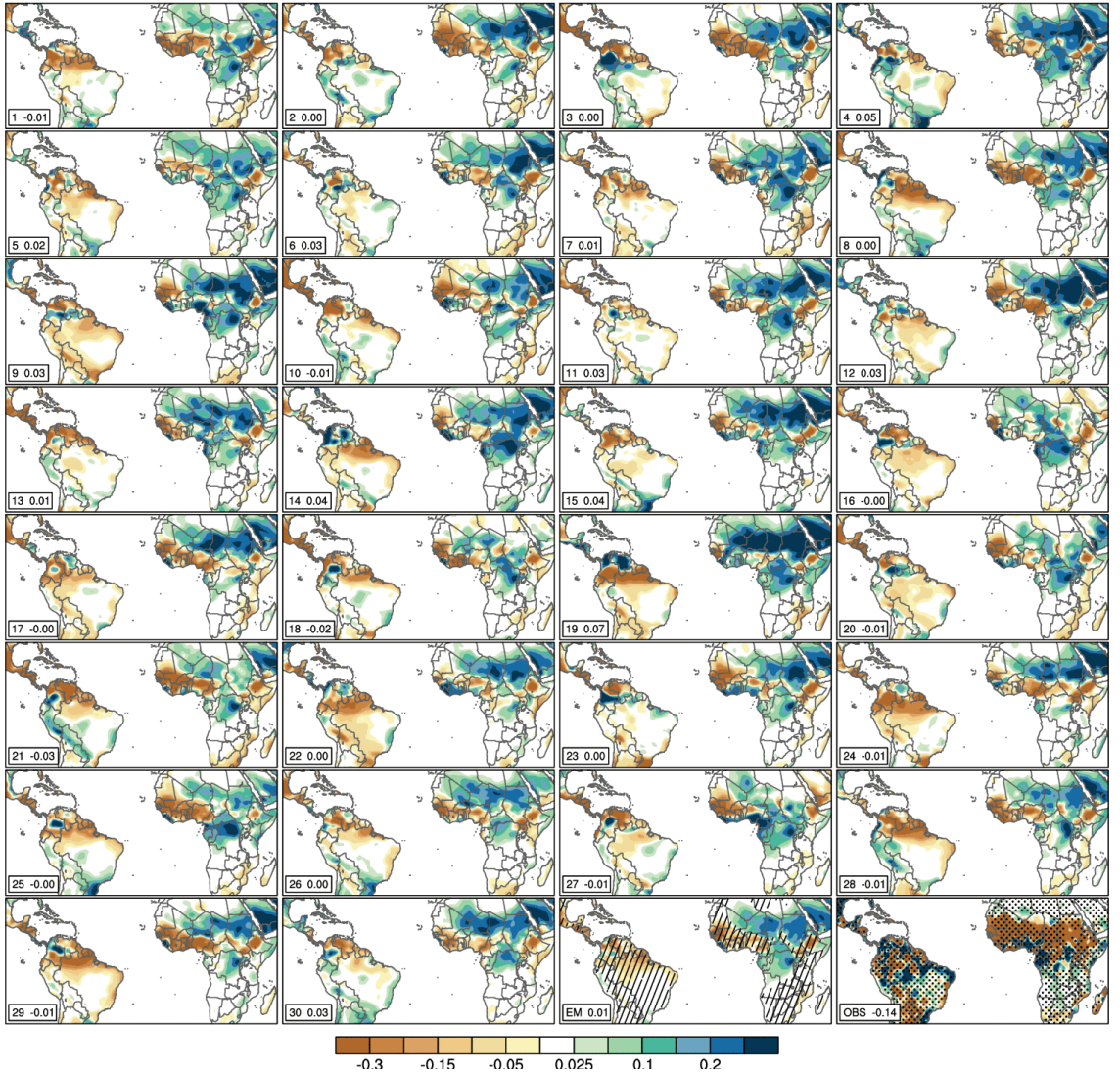


Figure 3. Same as Fig. 2 but for precipitation.

Figure 3 shows the same analysis for continental precipitation. The amplitude and even the sign of the 1950-2012 precipitation trend are very uncertain over many regions (see the hatching and stippling on the lower right panels of figure 3). This clearly suggests that the forced response in precipitation might not be detectable even when considering a

long-term trend. The central Sahel and eastern Africa show a forced response that is coherent in sign but with an amplitude less than 1.5 intra-ensemble standard deviation. Note also that the CESM-LE forced response indicates an increase of precipitation over these regions, contrasting with the large decrease seen in observations (we have used GPCC here) and analysed in many past studies. This indeed suggests that internal variability is the dominant driver of these past changes. The forced signal also shows a decrease along the Guinean coast, western Africa and in the northeast Brazil. The GPCC observations are much scattered over the northeast Brazil, making the inference more difficult. Future work will be directed a complete statistical analysis of the detection and attribution of anthropogenically-induced trends in presence of internal variability. Other climate variables than surface air temperature and precipitation will be considered as well.

b) Disentangling external forcings and internal variability is not straightforward because they are tightly linked as the external forcings affect the internal variability. Here we extend the analysis to 6 CMIP5 models, since the use of only one model can be misleading, because the representation of the forced versus internal variability can be a model-dependent feature. We show here that the respective roles of external forcings and internal variability in the long-term evolution of tropical Atlantic SSTs can be different for the different models. We have focused on the relative importance of the linear trend with respect of the residual variability, following the same methodology as in Doblas-Reyes et al 2013. For this, we have used simulations in hindcast mode (i.e. predictions, where the climate model is initialized from ocean and atmospheric reanalysis). By using predictions, we can disentangle whether the sources of predictability come mainly from the external forcing (climate linear trends) or from the internal or residual variability.

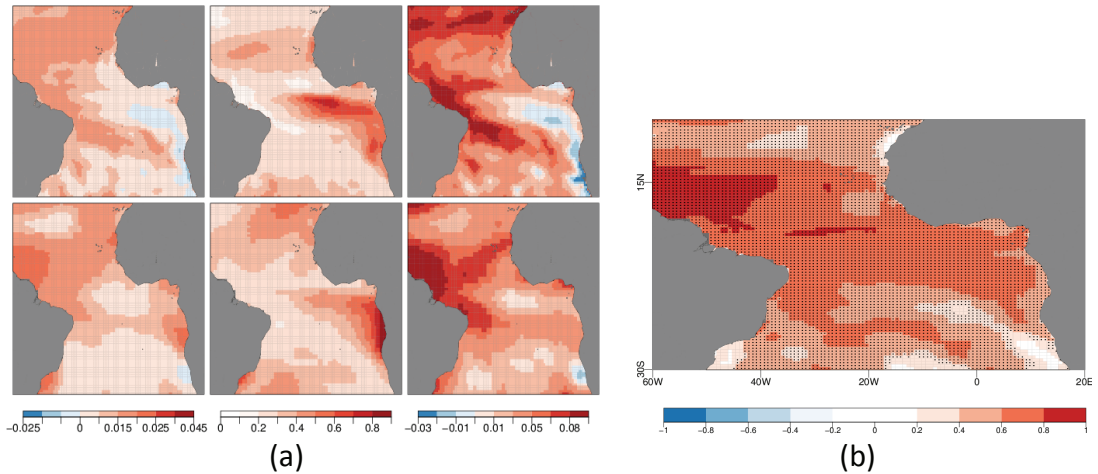


Figure 4. (a) Sea surface temperature summer (JJA) linear trend (first column), residual variability (second column) standard deviation, and ratio between the linear trend and the residual variability (third column). The first row shows the results with System4 data over 1981-2013, while the second row the results with ERSST data. (b) Summer sea surface temperature anomaly correlation coefficient of System4 with the ERSST data for the period 1981-2003. The black dots indicate the area where the skill is significant with 95% confidence according to a student t-test.

The first row of Figure 4a shows the results for the sea surface temperature (SST) in boreal summer (JJA) using the seasonal forecasts from ECMWF System4 initialized in May from 1981 to 2013, while the second row shows results for the ERSST data. The first column represents the SST linear trend, while the second column is the amplitude of the residual variability, calculated as the standard deviation of the detrended signal, and the third column is the ratio between the first two quantities (trend over residual variability ratio). Therefore the darker areas in the third column correspond either to the areas where the climate trend is strong, or where the residual variability is small. By looking at the observed trend (bottom left panel in figure 4a) we see that in the Angola-Benguela region there is a slightly cold trend in ERSST. System4 (top left panel in figure 4a) amplifies such a cold trend also in the Gulf of Guinea. The strongest warm trend in the observations is recorded along the coast of Brazil and is underestimated by System 4. The model captures the amplitude of the observed residual variability (central column in figure 4a) although both maxima, in the Gulf of Guinea and the subtropical North Atlantic, are in observations shifted respectively north-westward and eastward. Such a shift could explain the low skill (figure 1b) in the subtropical North Atlantic. By looking at the map of the anomaly correlation coefficient (figure 4b), we see that the region of maximum skill close to the Brazilian coast corresponds to the region where the ratio between the trend and the residual variability is the highest (third column in figure 4a) in both the model and the observations, due to the strong trend. Thus, the skill in this region arises from the model ability to capture the relatively strong trend. The region below 20°S, close to the coast does not have any skill probably due to the fact that there is a weak trend and a weak amplitude of the residual variability, while we have significant skill in the Gulf of Guinea as there is a good representation of the residual variability.

Model	No. members init prediction	No. members Historical	Period (1 start date per year)
MIROC5	6	1	1961-2011
HadCM3	10	10	1961-2010
EC-Earth v2.3	5	10	1961-2006
MPI (SPECS decadal)	5	3	1961-2012
GFDL-CM2	10	10	1961-2012
CANCM4	10	10	1961-2012

Table1.: CMIP5 decadal experiments used in the study, with the number of members and the covered period.

The same study has been repeated with the CMIP5 decadal experiments initialized every year on the 1st January. We have focused on the summer of the first forecast year. Each experiment covers a different period depending on the availability of the data (see Table 1 for details). Every member available for each experiment has been used. The analysis is carried out on the original grid of each experiment to reduce the impact of the interpolation.

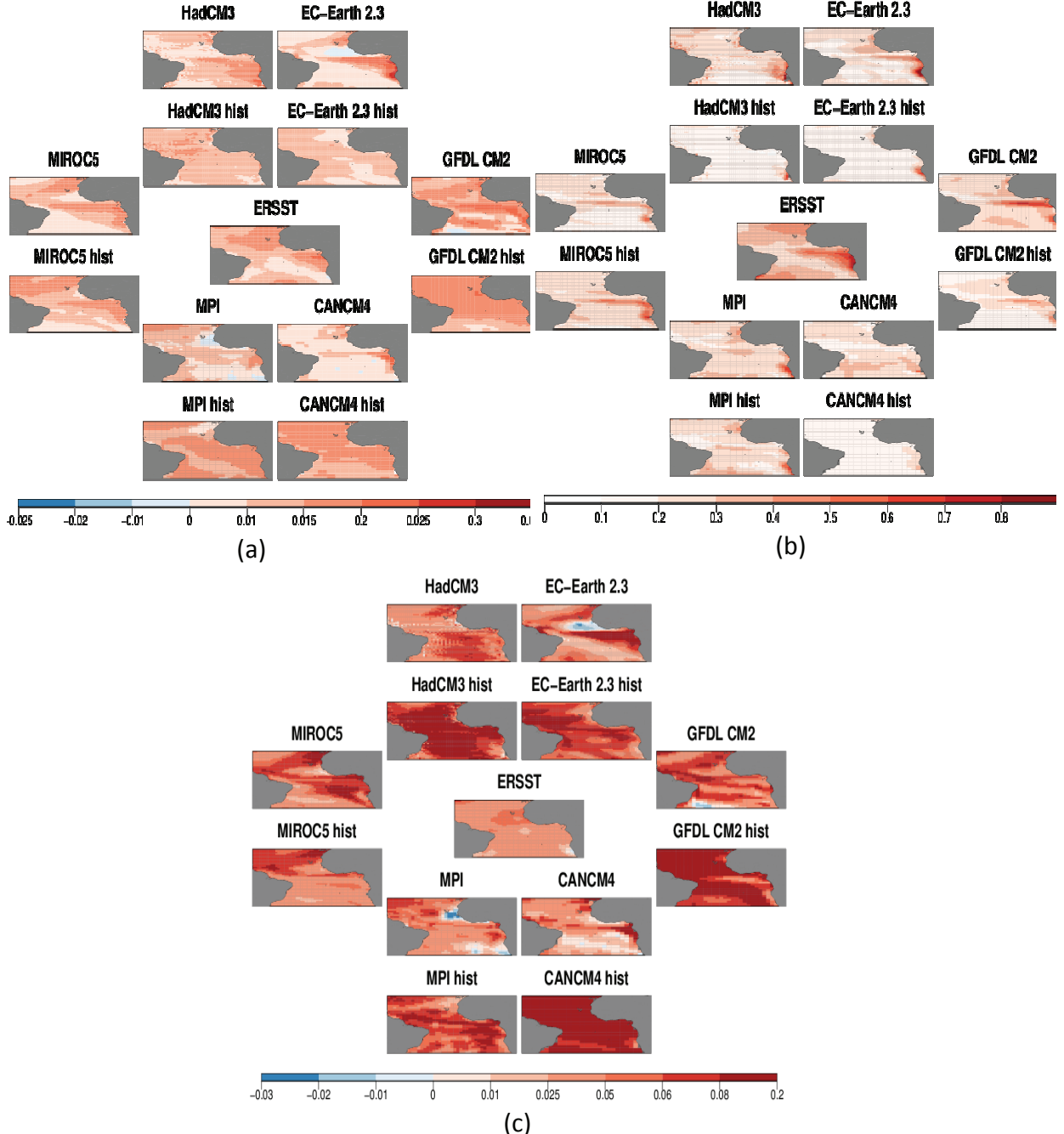


Figure 5. Trend (a), residual variability (b), and their ratio (c) of the JJA sea surface temperature over the period 1961–2006 (/2012, depending on the data available, see table 1). From the top, clockwise, HadCM3, EC-Earth 2.3, GFDL CM2, CANCM4, MPI and MIROC5 with the respective historical simulation (hist). In the center the trend calculated with the ERSST observed data using MIROC5 period of validation and resolution.

Figure 5a shows the linear trend of the summer SST, figure 5b the residual variability standard deviation and figure 5c the ratio. The measures are shown for both, the initialised hindcasts and the historical simulation (called hist or non-initialised). The central panel in each figure shows the measures (respectively the linear trend, the residual variability standard deviation and their ratio) calculated with the ERSST data.

As we saw before in figure 4a for the shorter period 1981-2013, the relative impact of the climate trend in the Angola-Benguela region is very small because of the weak SST trends in the region. The strongest relative impact of the observed trend is in the Northern subtropical Atlantic over the study region (figure 5c). The impact of the trend for the historical simulations is very strong because most of the interannual variability of the different members is filtered out with the ensemble mean (figure 5c). The initialisation results in more realistic SST trends, especially in HadCM3, GFDL-CM2 and MIROC5 but the observed pattern is not properly captured (figure 5a). The ratios of the SST linear trend and the amplitude of the residual variability in the subtropical North Atlantic of EC-Earth and MPI initialised simulations are worse than the historical simulations (figure 5c), because of the wrong negative trend introduced by the initialization (figure 5a). The major effect of the initialisation in terms of internal variability is the improvement of the Gulf of Guinea and the subtropical North Atlantic (figure 5b).

c) The AMV, which is closely connected to decadal variability in the TA region, has also shown impacts outside the Atlantic basin. In particular, several studies relate the positive (negative) phase of the AMV with a strengthening (weakening) of the Indian summer monsoon. However, Ting et al. (2011) show no connection between them in pre-industrial simulations and a weak positive relation in historical simulations, suggesting a possible role for the external forcing in mediating such relationship. In addition, the AMV could have an impact on global temperatures (Steinman et al. 2015). Here we investigate the connection of AMV with the Indian summer monsoon and the possible effect of external forcings through observation and CMIP5 models. We also look into the role of AMV in explaining the early 20th Century warming.

External forcing synchronizes the Atlantic Multidecadal Variability and the Indian Summer Monsoon

(Luo et al. 2015, submitted)

The relationship between the AMV and the Indian Summer Monsoon (ISM) is analysed using observations and reconstructed proxy records for the period 1720 to 1990. Indices of the two regions are significantly correlated ($R=0.61$) during the second half (1860-

1990) of the time series, while correlations are weaker and not significant before 1860 (Figure 6).

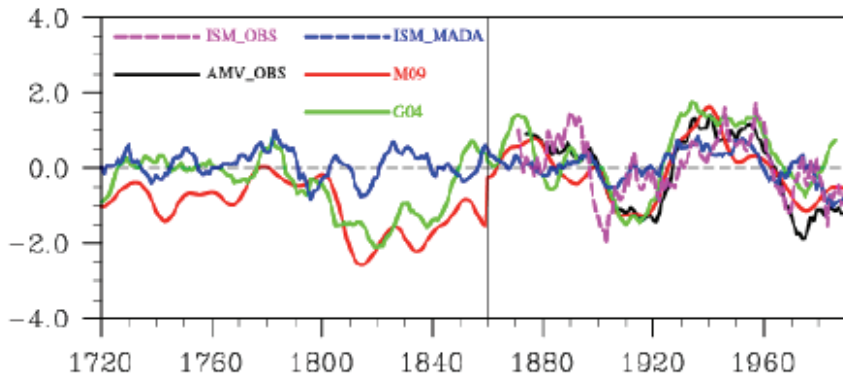


Figure 6. Temporal evolution of the AMV and ISM indices. Vertical solid line indicates the timing of 1860. AMV_OBS and ISM_OBS (black and pink line respectively come from HadISST dataset). M09 and G04 are the AMV reconstructions by Gray et al. 2004 and Mann et al. 2009, respectively. ISM_MADA is a reconstruction from the Monsoon Asia Drought Atlas.

The relationship is further analysed in twelve models from the CMIP5 that reasonably simulate both the AMV and the ISM. The enhanced post-1860's relation is not simulated by any of the models in Pre-industrial control simulations with fixed external forcing, but is reproduced by three models in historical simulations (1850-2005) with prescribed external forcings including the GHGs. Regression analyses reveal that external forcing is linked to mid-to-upper tropospheric temperature pattern with a strengthened land-ocean contrast in Southern Asia that is consistent with an enhanced ISM. External forcing also leads to a concurrent evolution of AMV. Thus, the significant relationship found in the observation after the onset of the industrial revolution may be associated with the external forcing, instead of resulting from internal climate dynamics.

Investigating the role of the Atlantic and Pacific in the early 20th century warming

(Svendsen et al., to be submitted)

We performed additional sensitivity studies with the Norwegian Earth System Model (NorESM) to further assess the global impacts of the AMV, and contrast it against Pacific Decadal Variability. We have performed four 6-member ensembles with NorESM with transient 20th century forcing. First we have a control ensemble (CNTRL) with 6 members of fully coupled historical simulations as done for the CMIP5. The other three ensemble simulations are partially coupled, similar to the setup from Ding et al., (2014): We prescribe daily momentum flux anomalies from the 20th Century Reanalysis (20CR; Compo et al., 2011) to the ocean component added to the daily climatology. This method is used to constrain the model variability to observations, while at the same time maintaining an active thermodynamic coupling. In the second ensemble (TAU) we prescribe the momentum flux globally at every grid point over the ocean, while in the third and fourth ensembles (TAU-ATL

and TAU-PAC) the prescribed momentum flux is only applied in the Atlantic and Indo-Pacific basins, respectively. With this experimental setup we are able constrain SST variability in the model to the observed, especially in the tropical Pacific.

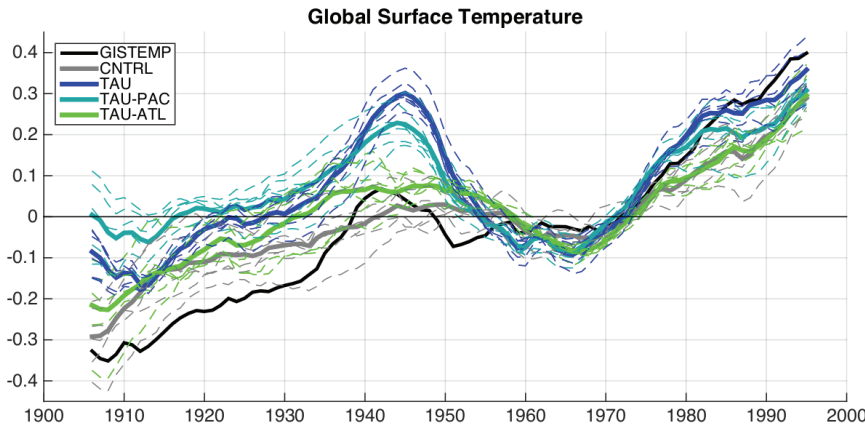


Figure 7. 11-year low-pass filtered global surface temperature for GISTEMP (black line) and the ensemble simulations. The ensemble means are the solid lines; dashed lines show the corresponding individual ensemble members.

3. Physical processes of long-term internal Tropical Atlantic variability

N. Keenlyside¹, E. Mohino², H. Nnamchi³, L. Svendsen⁴, J. Villamayor²

¹ UiB, Bergen, Norway

² UCM, Madrid, Spain

³ UNN, Nsukka, Nigeria

⁴ NERSC, Bergen, Norway

The internal variability is a result of complex interactions between components of the climate system (ocean, atmosphere, sea ice, continents). In this section we have been conducted analysis on observations, existing simulations (CMIP5 models) and numerical experiments performed in an idealised framework to identify mechanisms of low-frequency Tropical Atlantic variability over the ocean and the adjacent continents. Three papers have been finished on this issue and we presented a short summary below.

Extratropical origins of summer equatorial Atlantic decadal variability

(Nnamchi et al. 2015, in revision)

Estimates of periodicities of the Atlantic Niño from observations, theory and models generally fall within the inter-annual range of 1.6 to 4.5 years (Brandt et al 2011). However, a recent study suggests that the observed monthly equatorial Atlantic Niño index—defined as the SST anomalies averaged over 3N-3S, 0-20W—seemingly exhibits a decadal peak related to the southern subtropics (Nnamchi et al 2015). Here we show the seasonal and spatial realizations of the Tropical Atlantic Decadal Variability (TADV hereinafter) based on historical observations. Then, focusing on the boreal summer (June-July-August, JJA), we highlight the possible extra-tropical forcing of the equatorial decadal variability in the Atlantic Ocean.

To take into account the marked discrepancies that can exist among the globally complete reconstructed observational SST data sets (Deser et al 2010), we combined and analyzed historical SST fields from three different datasets. In our analysis, we have excluded the inter-annual and multi-decadal time scales by applying an 8–25 years Lanczos band-pass filter to each data set. The filtered data sets were analysed using empirical orthogonal function (EOF) and least-squares linear regression. Two seasons are considered MAM and JJA, the seasons with most pronounced decadal variability in the ATL3 Index (see figure 1 from Nnamchi et al. 2015).

In MAM, the TADV appears as an inter-hemispheric north-south SST gradient also known as the Atlantic Meridional Mode (AMM) (Carton et al 1996, Chang et al 1997, Ruiz-Barradas et al 2000, Chiang and Vimont 2004). The low-frequency variability SST mode for JJA is the Equatorial Mode (Zonal mode, Chang et al 2006; Keenlyside and Latif 2007), dominated by a strong equatorial zonal pattern and stronger wind anomalies over the South Atlantic Ocean. This equatorial Atlantic Decadal variability (EADV) explains around a 54% of the total variance in SSTs.

A further investigation of the decadal signature of the Equatorial Model reveals that the EADV is more related to ocean-atmosphere variability in the extratropical South Atlantic compared to the North Atlantic sector. In this context, the present study is essentially consistent with earlier observational and modelling studies. Figure 8 shows the North Atlantic (figure 8a) and South Atlantic (figure 8b) decadal variability patterns, obtained by applying EOFs analysis to the low-pass (8-25 years) filtered SSTs, and the regression of the PC1 for each EOF and the anomalies of geopotential height at 700 hPa (Z700). From figure 8a, we show that the EADV is strongly related to lower troposphere atmospheric variability over the South Atlantic and is characterized by an oscillation in the strength of the St. Helena subtropical anticyclone, which could induce equatorial SST variability via the wind-evaporation-SST feedback mechanism.

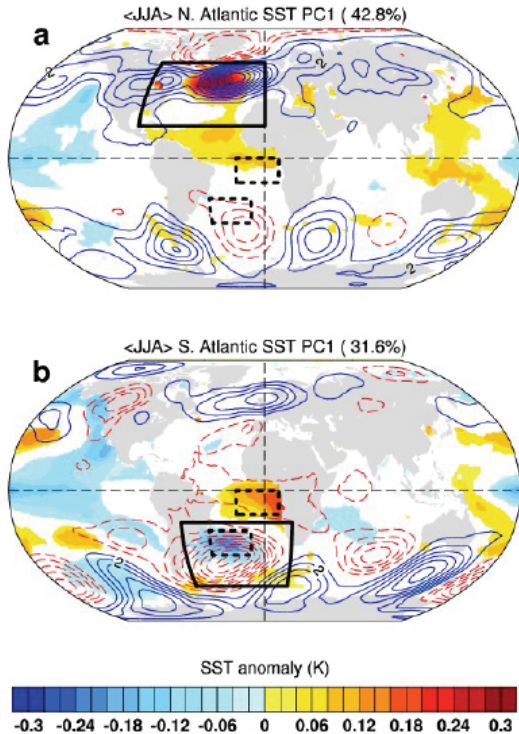


Figure 8. North Atlantic and South Atlantic decadal variability. Shading show the regressions of SST anomalies on the leading PC of the 8-25yr Lanczos band-pass filtered SST over the North Atlantic ($20N\text{--}60N$, $0\text{--}90W$) and South Atlantic ($20S\text{--}60S$, $20E\text{--}60W$) sectors. Dashed white boxes show the North-East-Pole ($0S\text{--}15S$, $20E\text{--}10W$) and South-West-Pole ($25\text{--}40S$, $10\text{--}40W$) of the SAOD. The variance (%) associated with the leading PC for the respective region is shown on the top right corner. Contours show the regression of Z700 anomalies (contours at intervals of $1m\text{-}1decade$) onto the leading PC of Z700 over the north (explained variance = 43.0%) and south (explained variance = 42.1%) Atlantic. Only statistically significant SST anomalies at $P \leq 0.001$ are shown (From Nnamchi et al. submitted).

Robust Sahel drought due to the Interdecadal Pacific Oscillation (IPO) in CMIP5 models (Villamayor J. and E.Mohino, 2015)

In this study, we have investigated the impact of the IPO on Sahel precipitation using the simulations from the CMIP5. We particularly address the following questions: (1) Is there an impact of the IPO on Sahel precipitation? (2) What is the dynamical mechanism for such impact? (3) How do coupled models simulate the IPO and its impact over the Sahel? (4) Does the radiative forcing affect this relationship?

We worked with the monthly data of SST, precipitation, and wind at high (200 hPa) and low (850 hPa) levels. To analyze the observed IPO and impacts, we use SST reconstructions from two different databases, precipitation from Climatic Research Unit time series version 3.1(CRU TS3.1) (Mitchell and Jones, 2005), and winds from the 20th Century Reanalysis (Compo et al., 2011). For the simulations, the output from 17 different CMIP5 models is used, previously interpolated to a common regular grid with a spatial

resolution of 2.8° in longitude and latitude. We have analyzed the unforced long-term preindustrial control (piControl) run, the historical run, which is a reproduction of the 20th century (typically from 1850 to 2005) with observed external forcing imposed, and the RCP8.5 future projection experiment, which considers the highest increase of anthropogenic gas concentration.

In order to isolate the internal variability of SSTs as much as possible, we remove the global component of the anthropogenic forcing in observations and forced simulations (Mohino et al. 2011). The IPO indices from observations and the forced simulations (historical and RCP8.5 experiments) are then defined as the first principal component (PC) of the residual SSTA, associated to the first empirical orthogonal function (EOF) calculated over the Pacific basin (between 60°N and 45°S).

Figure 9 shows the SST pattern associated with the IPO in the observations, historical and control simulations. From figure 9, the SST pattern in simulations (figure 9b-c) is consistent with observations (figure 9a). In the Pacific, there are cold anomalies over the western part of the basin, poleward of 25° and more prominent in the Northern Hemisphere. There are also warm anomalies over the tropical Pacific and over the north and south of the eastern part of the basin. The agreement among models on the SST pattern associated with the IPO is weaker in the historical runs than in the piControl ones.

Associated with a positive IPO, the models simulate a significant pattern of negative precipitation anomalies across the Sahel (figure 9b and 9c, low panel), in accordance with observations (figure 9a, low panel). Nevertheless, the observed positive anomalies of precipitation on the coastal area of Guinea, Sierra Leone, and Liberia are not reproduced in the simulations. Sahel drought in response to the IPO is a remarkably consistent feature across models and simulations. For both historical and piControl experiments, 13 out of the 17 models analyzed simulate a negative correlation between the IPO and the unfiltered Sahel precipitation index (not shown).

Investigating the physical mechanism leading to the IPO-Sahel drought teleconnections, in observations and simulations, a positive IPO is associated with anomalous convergence over the central tropical Pacific and divergence over the tropical Atlantic and West Africa at low levels. The response is reversed at high levels, showing anomalous divergence and convergence over these two regions, respectively (figure 4 from Villamayor and Mohino, 2015). This suggests an anomalous Walker-type overturning cell that connects upward movements over the central Pacific in response to local warm SSTAs there, with subsidence over West Africa. This, in turn, reduces the tropical easterly jet and the low-level monsoon westerlies, weakening the monsoon (not shown) and leading to drought conditions over the Sahel.

The similarity between the SSTA patterns of the historical and the unforced piControl simulations suggests that the IPO SST mode is mainly produced by the internal variability of the models and that radiative effects do not play a relevant role (figure 9 and figure 5 in Villamayor and Mohino, 2015).

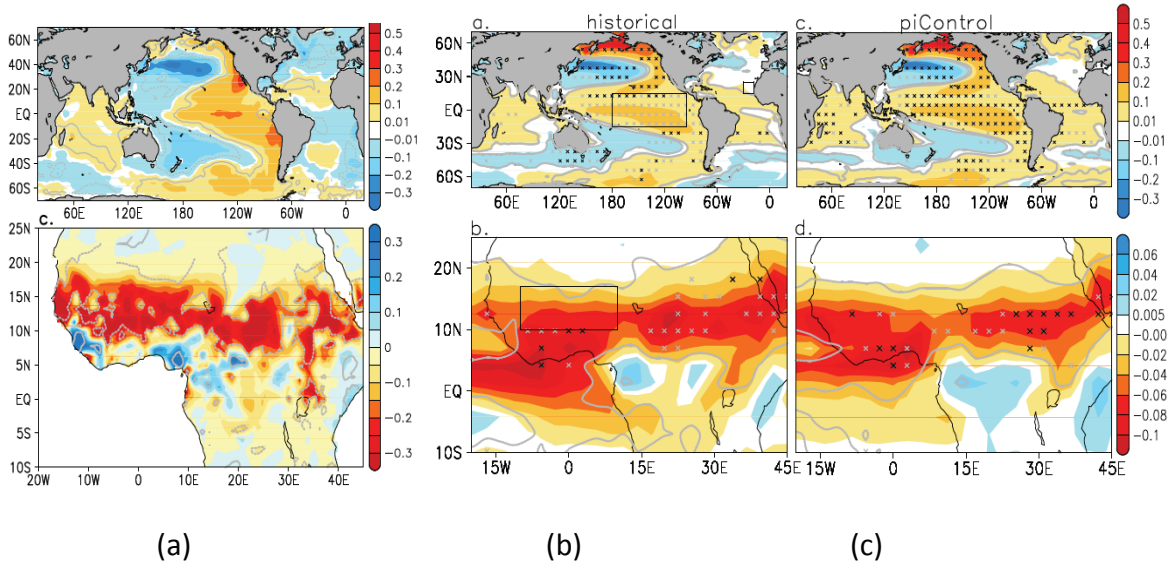


Figure 8. (a) Upper panel: Regression onto the IPO index of the unfiltered SST anomalies (K per standard deviation) and lower panel JAS precipitation anomalies (mm/d per standard deviation) in observations. (b) Upper panel: Regression onto the IPO index of the unfiltered SST anomalies (K per standard deviation) and lower panel JAS precipitation anomalies (mm/d per standard deviation) averaged over the 17 CMIP5 models in the historic run, typically from 1850 to 2005 (c) Same as Figures (b) but for the piControl run. The black and grey marks indicate the points where the regression coefficient sign coincides in at least 13 and 15 out of the 17 models analyzed, respectively. The grey contours indicate the regions where the averaged correlation is significant at alpha = 0.05 (using a Monte Carlo-based test). From Villamayor and Mohino, 2014.

Multiple timescales of stochastically forced North Atlantic Ocean variability: A model study

(Mecking et al. 2015)

Forced ocean model and coupled model experiments indicate that AMV results from internal climate dynamics (e.g., Delworth 1993, Knight et al. 2006, Eden and Jung, 2001, Mecking et al. 2013). Recently, several studies have suggested that external forcing may drive North Atlantic decadal variability either directly (e.g., Keenlyside et al., 2015) or by synchronization of internal modes of the climate system (Booth et al., 2012; Mann and Emanuel, 2006). Furthermore, in a recent study Mecking et al. 2015 have shown that stochastic atmospheric variability associated with the North Atlantic Oscillation (NAO) may explain a significant portion of AMV, through driving ocean circulation changes.

To investigate this, a 2000-year long global ocean model integration has been performed with the ocean model NEMO (Madec et al. 1998), forced with the atmospheric patterns associated with a white noise NAO index. The stochastic NAO forcing excited three distinct timescales of North Atlantic Ocean variability, whose prints that can be observed in the Atlantic Meridional Overturning Circulation (AMOC) and SubPolar Gyre (SPG) strength.

Figure 10 shows the power spectrum for the AMOC (figure 10a) and SPG (figure 10b) for this idealized experiment. First, an interannual timescale with variability shorter than 15

years, that is related to Ekman dynamics (red line). Second, a multi-decadal timescale, on the 15 to 65 year range (green line), that is mainly concentrated in the SPG region and is controlled by constructive interference between density anomalies and the changing NAO forcing. Finally, a centennial timescales, with variability longer than 65 years (blue line), that results from the ocean being in a series of quasi-equilibrium states.

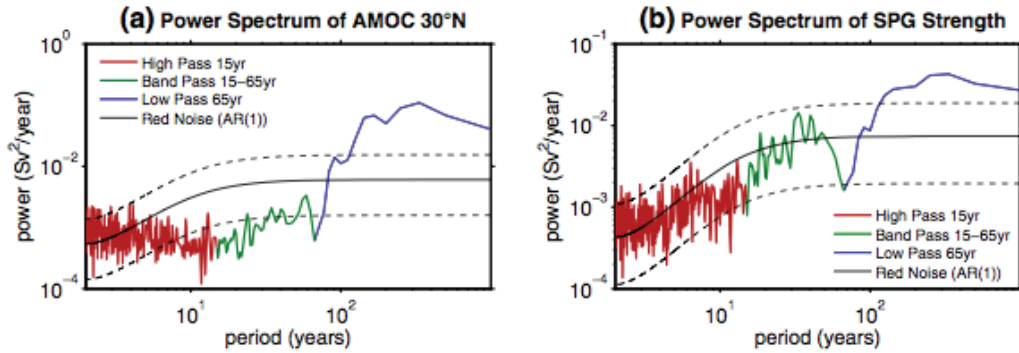


Figure 9. The power spectrum of (a) the AMOC at 30°N and (b) the SPG Strength, divided into periods of 15 years or less (red), 15–65 years (green) and 65 years and longer (blue). The AR(1) fit is shown in black with dashed lines indicated the 95 % confidence interval. From Mecking et al. 2015.

The relationship between the ocean's response and the NAO index differs for each timescale; the 15-year and shorter timescales are directly related to the NAO of the same year, 15- to 65-year timescales are dependent on the NAO index in the last 25–30 years in a sinusoidal sense while the 65-year and longer timescales relate to a sum of the last 50–80 years of the NAO index.

References:

In bold blue the PREFACE (D9.2) references

Booth, B. B. B., N. J. Dunstone, P. R. Halloran, T. Andrews, and N. Bellouin, 2012: Aerosols implicated as a prime driver of twentieth-century North Atlantic climate variability, *Nature*, 484, 228–232.

Brandt P, Funk A, Hormann V, Dengler M, Greatbatch R J and Toole J M, 2011: Interannual atmospheric variability forced by the deep equatorial Atlantic Ocean, *Nature*, 473, 497–500

Carton J A, Cao X, Giese B S and Da Silva A M, 1996 : Decadal and interannual SST variability in the tropical Atlantic Ocean, *J. Phys. Oceanogr.*, 26 1165–1175

Chang, P., Ji, L., Li, H., 1997: A decadal climate variation in the tropical atlantic ocean from

thermodynamic air-sea interactions, *Nature*, 385(6616), 516–518

Chang P, Fang Y, Saravanan R, Ji L and Seidel H, 2006 : The cause of the fragile relationship between the Pacific El Niño and the Atlantic El Niño, *Nature*, 443 324-328

Chiang J. C. and D.J. Vimont, 2004: Analogous Pacific and Atlantic Meridional Modes of Tropical Atmosphere–Ocean Variability, *J. Climate*, 17, 4143-4158.

Compo, G. P., et al., 2011: The Twentieth Century Reanalysis Project, *Q. J. R. Meteorol. Soc.*, 137, 1–28, doi:10.1002/qj.776.

Deser C, Phillips A S and Alexander M A, 2010 : Twentieth century tropical sea surface temperature trends revisited ,*Geophys. Res. Lett.*, 37 L10701

Deser, C., A. S. Phillips, V. Bourdette, and H. Teng, 2012: Uncertainty in climate change projections: The role of internal variability. *Clim. Dyn.*, 38, 527-546, doi: 10.1007/s00382-010-0977-x

Ding, H., R. Greatbatch, W. Park, M. Latif, V. Semenov, and X. Sun, 2014: The variability of the East Asian summer monsoon and its relationship to ENSO in a partially coupled climate model. *Clim. Dyn.*, 42(1-2), 367-379, doi: 10.1007/s00382-012-1642-3

Doblas-Reyes F. J., I. Andreu-Burillo, Y. Chikamoto, J- García-Serrano, V. Guemas, M. Kimoto, T. Mochizuki, L. R. L. Rodrigues and G. J. van Oldenborgh, 2013: Initialized near-term regional climate change prediction. *Nat. Commun.*, 4, doi: 10.1038/ncomms2704.

Goldenberg, S. B., C. W. Landsea, A. M. Mestas-Nunez, and W. M. Gray, 2001 : The recent increase in Atlantic hurricane activity: Causes and implications, *Science*, 293(5529), 474–479, doi:10.1126/science.1060040.

Gray, S. T., L. J. Graumlich, J. L. Betancourt, and G. T. Pederson, 2004 : A tree-ring based reconstruction of the Atlantic Multidecadal Oscillation since 1567 AD, *Geophys. Res. Lett.*, 31, L12205, doi:10.1029/2004GL019932.

IPCC, (2007): Climate Change 2007, The Physical Science Basis. Contribution of Working Group 1 to the Fourth Assessment Report on the Intergovernmental Panel on Climate Change, edited by S. Solomon et al., 996 pp., Cambridge Univ. Press, Cambridge, U.K.

IPCC, (2013): Climate Change 2013: The Physical Science Basis. Contribution of Working Group I to the Fifth Assessment Report of the Intergovernmental Panel on Climate Change [Stocker, T.F., D. Qin, G.-K. Plattner, M. Tignor, S.K. Allen, J. Boschung, A. Nauels, Y. Xia, V. Bex and P.M. Midgley (eds.)]. Cambridge University Press, Cambridge, United Kingdom and New York, NY, USA, 1535 pp, doi:10.1017/CBO9781107415324.

Kay, J. E., C. Deser, A. Phillips, A. Mai, C. Hannay, G. Strand, J. Arblaster, S. Bates, G. Danabasoglu, J. Edwards, M. Holland, P. Kushner, J. -F. Lamarque, D. Lawrence, K. Lindsay, A. Middleton, E. Munoz, R. Neale, K. Oleson, L. Polvani, and M. Vertenstein, 2014: The

Community Earth System Model (CESM) Large Ensemble Project: A community resource for studying climate change in the presence of internal climate variability. Bull. Amer. Met. Soc., in press, doi: 10.1175/BAMS-D-13-00255.1.

Keenlyside, N.S., Latif, M., 2007: Understanding equatorial atlantic interannual variability. J. Climate 20, 131–142, URL <http://dx.doi.org/10.1175/JCLI3992.1>

Keenlyside, N. S., J. Ba, J. Mecking, N.-O. Omrani, M. Latif, R. Zhang, and R. Msadek, 2015: North Atlantic multi-decadal variability - mechanisms and predictability. *Climate Change: Multidecadal and Beyond*, C.-P. Chang, M. Ghil, M. Latif, and M. Wallace, Eds., World Scientific Publishing Company, Singapur, n/a. ISBN 978-9814579926.

Luo F., Y. Gao, L. Svendsen, N. Keenlyside, S. Li and T. Furevik, 2015: External forcing synchronizes the Atlantic Multidecadal Variability and the Indian Summer Monsoon. Submitted to J. Climate

Madec G, Delecluse P, Imbard M, Levy C, 1998 : Opa 8.1 ocean general circulation model reference manual. Note du Pole de modelisation. Institut Pierre-Simon Laplace:11

Mann, M. E., Z. H. Zhang, S. Rutherford, R. S. Bradley, M. K. Hughes, D. Shindell, C. Ammann, G. Faluvegi, and F. B. Ni, 2009 : Global signatures and dynamical origins of the Little Ice Age and Medieval Climate Anomaly, Science, 326(5957), 1256–1260, doi:10.1126/science.1177303.

Mann, M. E. and K. A. Emanuel, 2006: Atlantic Hurricane Trends Linked to Climate Change. Eos Trans. AGU, 87, 233.

Martín-Rey M, Rodriguez-Fonseca B., Polo I., Kucharski F., 2014: On the Atlantic-Pacific Niños connection: a multidecadal modulated mode, Clim., Dyn., 43(11). DOI:10.1007/s00382-014-2305-3

Mecking, J., N. Keenlyside, and R. Greatbatch, 2015: Multiple timescales of stochastically forced North Atlantic Ocean variability: A model study. Ocean Dynamics, 1-15.

Mitchel, T. D., and P. D. Jones, 2005: An improved method of constructing a database of monthly climate observations and associated high-resolution grids, Int. J. Climatol., 25, 693–712, doi:10.1002/joc.1181.

Mohino, E., S. Janicot, and J. Bader, 2011: Sahel rainfall and decadal and multi-decadal sea surface temperature variability, Clim. Dyn., 37, 419–440, doi:10.1007/s00382-010-0867-2.

Nnamchi H C, Li J, Kucharski F, Kang I-S, Keenlyside N S, Chang P and Farneti R, 2015 : The Atlantic Niño—an equatorial arm of the South Atlantic Ocean dipole. Manuscript submitted to J. Clim.

Nnamchi H., Li J., Kucharski F., Keenlyside No. And Chang P., 2015 : Extratropical origins of

summer equatorial Atlantic decadal variability, submitted to Environmental Research Letters.

Rayner, N. A., D. E. Parker, E. B. Horton, C. K. Folland, L. V. Alexander, D. P. Rowell, E. C. Kent, and A. Kaplan, 2003 : Global analyses of sea surface temperature, sea ice, and night marine air temperature since the late nineteenth century, *J. Geophys. Res.*, 108(D14), 4407, doi:10.1029/2002JD002670.

Ruiz-Barradas, A., Carton, J.A., Nigam, S., 2000 : Structure of interannual-to-decadal climate variability in the tropical atlantic sector. *Am. Met. Soc.*, 13 , 3285-3297

Steinman, B.A., M.E. Mann and S.K. Miller, 2015 : Atlantic and Pacific multidecadal oscillations and Northern Hemisphere temperatures. *Science*, 347, 988-991, doi: 10.1126/science.1257856

Svendsen, L., S. Hetzinger, N. Keenlyside, and Y. Gao, 2014: Marine-based multiproxy reconstruction of Atlantic multidecadal variability, Geophys. Res. Lett., 41, 1295–1300, doi:10.1002/2013GL059076.

Svendsen, L., N. Keenlyside, I. Bethke and Y. Gao, 2015: Investigating the role of the Atlantic and Pacific in the early 20th century warming, to be submitted

Taylor, K. E., R. J. Stouffer, and G. A. Meehl, 2012 : An overview of CMIP5 and the experiment design, *Bull. Am. Meteorol. Soc.*, 93, 485–498.

Ting, M., Y. Kushnir, R. Seager, and C. Li, 2011 : Robust features of Atlantic multi-decadal variability and its climate impacts. *Geophys. Res. Lett.*, 38, L17705, doi: 10.1029/2011GL048712.

Tokinaga, H., and S.-P. Xie, 2011: Weakening of the equatorial Atlantic cold tongue over the past six decades. *Nature Geosci.*, 4, 222-226; advance online publication, 6 February 2011 (doi:10.1038/ngeo1078)

Villamayor J. and E. Mohino, 2015 : Robust Sahel drought due to the Interdecadal Pacific Oscillation in CMIP5 simulations, Geophys. Res. Lett., 42, 1214–1222, doi: 10.1002/2014GL062473.

Wang, C. Z., S. F. Dong, A. T. Evan, G. R. Foltz, and S. K. Lee, 2012 : Multidecadal covariability of North Atlantic sea surface temperature, African dust, Sahel rainfall, and Atlantic hurricanes, *J. Clim.*, 25(15), 5404–5415, doi:10.1175/jcli-d-11-00413.1.

Zhang, R., and T. L. Delworth, 2006 : Impact of Atlantic multidecadal oscillations on India/Sahel rainfall and Atlantic hurricanes, *Geophys. Res. Lett.*, 33, L17712, doi:10.1029/2006GL026267.